Journal of Hazardous Materials 505 (2026) 141412

Contents lists available at ScienceDirect

Journal of Hazardous Materials

journal homepage: www.elsevier.com/locate/jhazmat

Cadmium disrupts energy metabolism in the Harmonia axyridis via mediating trehalose metabolism pathway: A multi-omics analysis

Shasha Wang [a,b], Sijing Wan [a], Qintian Shen [a], Lei Yue [d], Jie Wang [a], Min Zhou [a], Yan Li [a,c,*], Bin Tang [a,**]

[a] College of Life and Environmental Sciences, Hangzhou Normal University, Hangzhou, Zhejiang 311121, China
[b] Zhejiang University, Hangzhou, Zhejiang 310058, China
[c] Tianjin Medical University, Tianjin 300070, China
[d] School of Life Sciences, Hebei University, Baoding, Hebei 071002, China

HIGHLIGHTS

- Cd toxicity (LC_{50}) in *Harmonia axyridis* larvae involves dose-dependent transcriptional and metabolic changes.
- Multi-omics links Cd toxicity to disrupted trehalose metabolism, with carbohydrate accumulation and enzyme/gene dysregulation.
- Food chain Cd transfer from soil to ladybugs disrupts energy balance, revealing a pathway harming natural pest control.

GRAPHICAL ABSTRACT

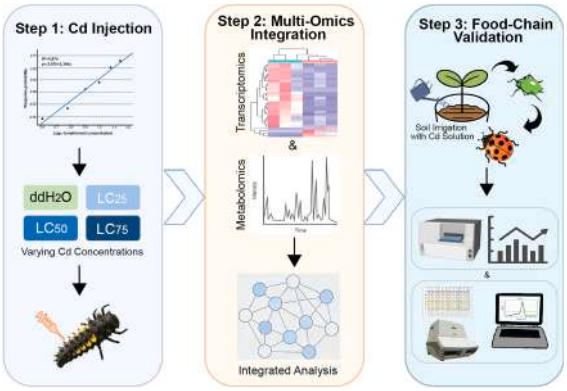

ARTICLE INFO

Keywords:
Cadmium
Harmonia axyridis
Transcriptomics
Metabolomics
Trehalase

ABSTRACT

Cadmium (Cd), a ubiquitous heavy metal pollutant, threatens the ecological functions of the natural enemy insect *Harmonia axyridis*, though the molecular mechanisms of its toxicity remain poorly understood. Here, we first determined the 48-h median lethal concentration (LC_{50}) of Cd for third-instar *H. axyridis* larvae as 7.667 mg/mL. Using a multi-omics approach, we then analyzed larval responses to injected Cd stress at LC_{25}, LC_{50}, and LC_{75} concentrations. Transcriptomics revealed 1986, 1471, and 1433 differentially expressed genes (DEGs) in the respective treatment groups, including down-regulated genes encoding α,α-trehalase (TRE) and maltase-glucoamylase involved in carbohydrate metabolism. Metabolomics identified 907, 294, and 511 differential metabolites (DMs) across the three Cd exposures, with significant accumulation of sucrose and sucrose 6′-phosphate in the LC_{50} group. Integrated omics analysis showed that both DEGs and DMs were co-enriched in starch and sucrose metabolism and galactose metabolism pathways. Furthermore, Cd transferred through the soil-plant-aphid-ladybug food chain disrupted trehalose metabolism, leading to reduced carbohydrate levels, suppressed

* Corresponding author at: College of Life and Environmental Sciences, Hangzhou Normal University, Hangzhou, Zhejiang 311121, China.
** Corresponding author.
E-mail addresses: jlyk@hznu.edu.cn (Y. Li), tbzm611@hznu.edu.cn (B. Tang).

https://doi.org/10.1016/j.jhazmat.2026.141412
Received 25 September 2025; Received in revised form 5 February 2026; Accepted 6 February 2026
Available online 18 February 2026

trehalase activity, and altered expression of key metabolic genes. Together, these results indicate that Cd-induced downregulation of trehalose-related genes causes upstream carbohydrate accumulation (e.g., sucrose) and disrupts the trehalose metabolic pathway, ultimately impairing energy homeostasis. This study uncovers a novel mechanism by which heavy metal pollution affects natural enemy insects via metabolic interference. Our findings highlight the potential disruption of pest control in agroecosystems under heavy metal stress and provide critical molecular targets for assessing the ecological risk of Cd pollution on beneficial insects.

1. Introduction

With the rapid industrialization and intensive agriculture, heavy metal pollution, particularly has emerged as a critical environmental challenge in agricultural ecosystems, severely threatening soil health, food safety, and biological control functions [1]. As a non-essential, non-biodegradable element, Cd exhibits high toxicity, strong mobility, persistence, and pronounced bioaccumulation [2]. It enters the environment through natural processes such as erosion and human activities including zinc refining, battery manufacturing, and application of phosphate fertilizers containing Cd residues, and spreads via atmospheric emissions, wastewater, and solid waste (Burden 2019). In farmlands, Cd readily accumulates in crops and transfers through the food chain, posing risks not only to crop quality and yield but also to the ecological functions of insects at different trophic levels.

The toxic effects of Cd on insects are widespread and trophically transmitted. It first accumulates in plants, then transfers to primary consumers through feeding, and further bioaccumulating in higher trophic predators, ultimately disrupting the balance of agricultural ecosystems [3,4]. Research have shown that Cd stress universally interferes with insect energy metabolism, which is a core physiological process sustaining growth, reproduction, and survival. Specifically, Cd exposure reduces metabolic rates and energy consumption, inhibits the expression of key genes in glycolysis and carbohydrate metabolism pathways, and impairs energy supply [5,6]. For pollinators like *Bombus* spp. such energy metabolism disorders directly lead to reduced flight ability [2]. For natural enemy insects, Cd-induced toxicity manifests as growth retardation, reduced survival rates, weakened fecundity and morphological abnormalities. These effects have been reported in *H. axyridis*, *Trichogramma*, and *Cryptolaemus montrouzieri* ([7,8] ; [9,10]). However, most existing studies focus on herbivorous or pollinating insects; research on predatory natural enemies remains limited, especially regarding molecular mechanisms underlying energy metabolism disruption.

In agricultural ecosystems, the transfer of Cd through the "plant–herbivorous insect–predatory insect" trophic chain represents a classic pathway for heavy metal translocation along the food web. Broad beans (*Vicia faba* L.) efficiently accumulate Cd and exhibit tolerance to moderate Cd stress [11]. The aphid (*Megoura crassicauda*), a primary pest of broad beans, accumulates Cd by feeding on the phloem sap of contaminated plants [12]. As a key aphid predator, *Harmonia axyridis* is vital for regulating aphid populations and maintaining balance in agricultural ecosystems [13]. However, while heavy metal transfer from aphids to ladybirds via predation has been reported [14,15], its molecular consequences, particularly on energy metabolism, remain poorly understood. Current toxicity studies on natural enemies largely focus on heavy metal accumulation and phenotypic endpoints, leaving significant mechanistic gaps unaddressed [16,17].

Specifically, three critical research lacunae persist: (1) a predominant emphasis on phenotypic effects with limited insight into underlying metabolic mechanisms; (2) unclear concentration-dependent responses of insect sugar metabolism under Cd stress; and (3) an unexplored role of the trehalose metabolism pathway in Cd stress adaptation. To address these gaps, this study investigates Cd toxicity in *H. axyridis* larvae through an integrated ecotoxicological and multi-omics approach. We aim to determine the acute toxicity of Cd exposure, identify the metabolic pathways perturbed by Cd through integrated transcriptomic and metabolomic analyses, and dissect the trehalose metabolism pathway by tracking the dynamic changes in related gene expression, enzyme activity, and carbohydrate content. By integrating cadmium injection-based omics analysis with food-chain exposure validation, this study seeks to elucidate the molecular basis of Cd toxicity in a key predatory insect, thereby providing insights for assessing ecological risks of heavy metal pollution in agricultural systems.

2. Materials and methods

2.1. Plant material and insect sources

The broad bean cultivar used in this experiment was Qingchan No. 14, and the aphids (*M. crassicauda*) employed in the experiments were a long-term, purified clonal population maintained in the laboratory, and reared on healthy broad bean seedlings that were free of heavy metal contamination. The *H. axyridis* colony was initially collected from the campus of Hangzhou Normal University and surrounding farmlands. Subsequently, a stable laboratory colony was established by rearing these lady beetles on pea aphids under standard conditions. Feeding conditions were maintained at a temperature of 25 ± 1°C, relative humidity of 70 ± 5 %, and a photoperiod of 14 h light:10 h dark (14 L:10D). Offspring of this laboratory colony were used in all experiments to minimize variations in genetic background and prior exposure history among test individuals.

2.2. Determination of median lethal concentration

$CdCl_2$ was dissolved in sterile double-distilled water (ddH_2O) to prepare a series of Cd^{2+} stock solutions (4, 6, 8, 10, 12, and 14 mg/mL). Third-instar *H. axyridis* larvae of uniform size were selected for the toxicity bioassay. To distinguish mortality caused by mechanical injury from that induced by Cd toxicity, a preliminary injection of 100 nL sterile ddH_2O was performed using a microinjector (Nanoject II/III) dorsally into the third abdominal segment. Larvae that died within 2 h post-injection were considered casualties of the injection procedure and excluded from subsequent analyses. For the formal toxicity test, larvae were injected with 100 nL of each Cd^{2+} solution at the designated concentrations, while the control group received 100 nL sterile ddH_2O. Mortality was recorded at 48 h post-injection. The median lethal concentration (LC_{50}) and the lethal concentrations for 25 % and 75 % of the population (LC_{25} and LC_{75}) were determined using probit analysis in SPSS v26 software.

2.3. Total RNA isolation and cDNA synthesis

Total RNA was extracted from whole third-instar larvae at 48 h post-injection with Cd^{2+} solutions corresponding to the LC_{25}, LC_{50}, or LC_{75} concentrations, using TRIzol reagent (Invitrogen, USA). RNA integrity was confirmed by 1 % (w/v) agarose gel electrophoresis, and its concentration and purity were determined using a NanoDrop 2000 spectrophotometer (Thermo Fisher Scientific, USA). Following treatment with DNase I to remove genomic DNA contamination, cDNA was synthesized from the purified RNA using the PrimeScript RT Reagent Kit with gDNA Eraser (Takara Bio, Japan) in accordance with the manufacturer's instructions.

Cd chloride solutions at LC_{25}, LC_{50}, and LC_{75} concentrations, as well as

ddH₂O (control), were selected for larval microinjection to conduct transcriptome and metabolome sequencing analyses. A completely randomized design was adopted for the experiment: uniform in size, healthy and active third-instar larvae were randomly assigned to four treatment groups (control, LC_{25}, LC_{50}, LC_{75}). For both transcriptomic and metabolomic analyses, each treatment group consisted of pools of 10 third-instar larvae per replicate. Transcriptomic sequencing was performed with 3 biological replicates per group, while metabolomic analysis was conducted with 6 biological replicates per group. The detailed experimental design is shown in Fig. 1A. RNA sequencing was performed by BGI Genomics (Beijing, China).

2.4. Transcriptome analysis

Adapter sequences and low-quality reads were removed from raw data to generate clean reads. De novo transcriptome assembly produced unigenes, which were functionally annotated using BLAST against NCBI non-redundant (Nr) databases. Gene expression was quantified as FPKM (fragments per kilobase per million mapped reads) with RSEM. Differential expression analysis used DESeq2 and results were visualized in volcano plots. Differentially expressed genes (DEGs) were selected based on the thresholds of an absolute log2(fold change) ≥ 1 and a false discovery rate (FDR) < 0.05.For the DEGs, enrichment analysis was carried out utilizing the Gene Ontology (GO) database (http://www.geneontology.org/) and the Kyoto Encyclopedia of Genes and Genomes (KEGG) database (https://www.genome.jp/kegg). Significant GO terms (with FDR < 0.05) and KEGG pathways (with $P < 0.05$) were identified by means of hypergeometric tests. Weighted gene co-expression network analysis (WGCNA) was performed to identify clusters of highly correlated genes and to investigate their association with cadmium treatment. Genes with low expression (FPKM < 1) were filtered out, retaining 12,458 high-quality genes for subsequent analysis. Based on the scale-free network criterion ($R^2 > 0.85$), the soft-thresholding power β was determined to be 8. Using the dynamic tree cut algorithm (minModuleSize = 30, mergeCutHeight = 0.25), genes were clustered into 21 co-expression modules. The "Cd treatment concentration (LC_{25}, LC_{50}, LC_{75})" was used as the phenotypic trait, and Pearson correlation coefficients were calculated between each module and the trait. Within the MEroyalblue module, hub genes were identified by filtering for Gene Significance (GS > 0.5) and Module Membership (MM > 0.8).

2.5. Untargeted metabolome analysis

Third-instar larvae were injected with Cd^{2+} at LC_{25}, LC_{50}, or LC_{75} concentrations, and samples were collected 48 h post-injection for LC-MS/MS analysis. The analysis was performed using a liquid chromatography-tandem mass spectrometry (LC-MS/MS) platform with the following optimized parameters: Chromatographic conditions: An Agilent ZORBAX SB-C18 column (2.1 mm × 100 mm, 1.8 μm) was used for separation. The mobile phase consisted of Phase A (0.1 % formic acid in water) and Phase B (0.1 % formic acid in acetonitrile). The gradient elution program was set as follows: 5 % B from 0 to 2 min; linear gradient from 5 % to 95 % B from 2 to 10 min; maintained at 95 % B from 10 to 12 min; rapid re-equilibration from 95 % to 5 % B within 0.1 min (12–12.1 min); and held at 5 % B from 12.1 to 15 min for column stabilization. The flow rate was 0.3 mL/min, column temperature was controlled at 40℃, and the injection volume was 2 μL. Mass spectrometric conditions: An electrospray ionization (ESI) source was used in both positive and negative ion modes. The mass scanning range was set to *m/z* 50–1000, and the collision energy was adjusted between 10–40 eV to enhance metabolite fragmentation.

Metabolite annotations were retrieved from multiple metabolome

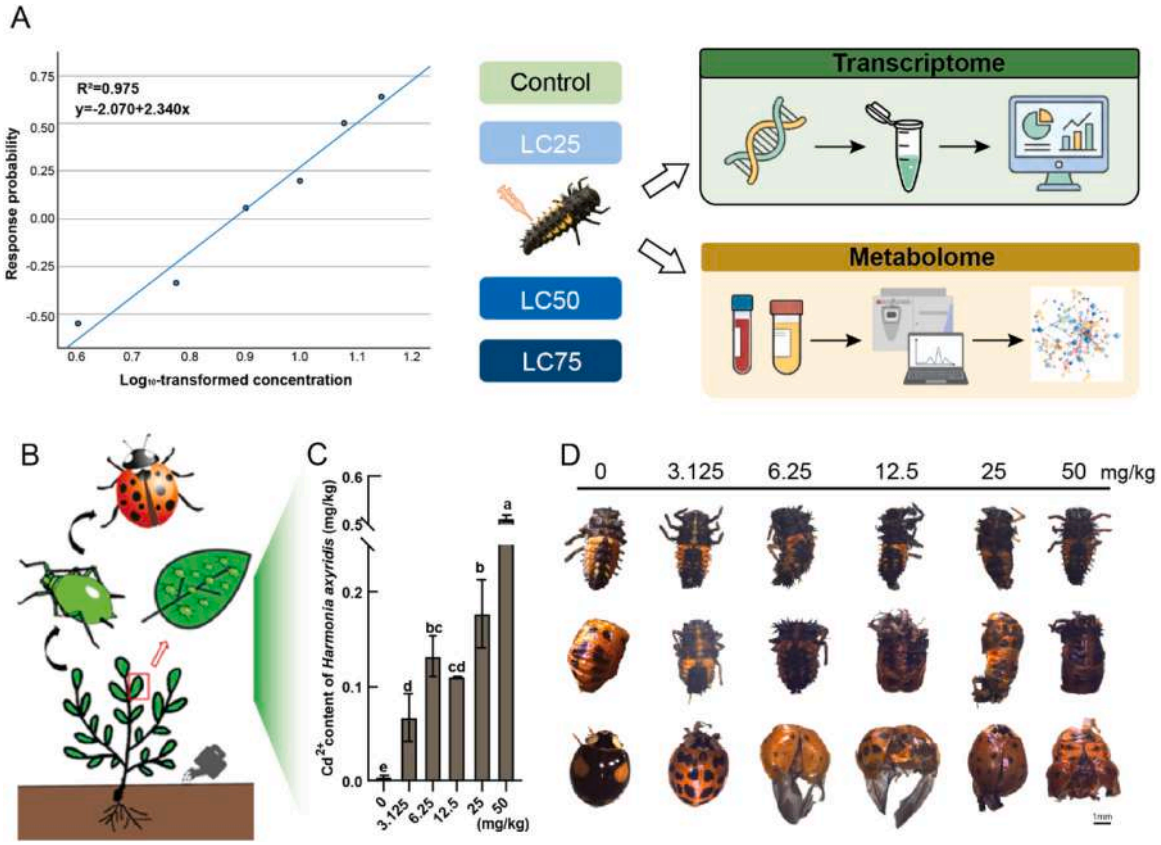

Fig. 1. Overview of the integrated study on cadmium (Cd) toxicity in *H.axyridis*. (A) Schematic workflow of the multi-omics study on Cd toxicity in *H. axyridis*. (B) Experimental design for Cd transfer along a soil-plant-aphid-ladybug food chain. (C) Cadmium accumulation in *H. axyridis* across different treatments. (D) Phenotypic abnormalities in *H. axyridis* induced by cadmium (Cd) exposure.

databases, including the laboratory's in-house database, integrated public repositories. To characterize metabolic profile differences across groups, principal component analysis (PCA) and orthogonal partial least squares discriminant analysis (OPLS-DA) were performed. The OPLS-DA models were validated via permutation tests, with R^2 and Q^2 values serving as metrics to evaluate model fitness. Differentially metabolites (DMs) were defined by the criteria: FDR < 0.05, variable importance in projection (VIP) > 1, and fold change either > 2 or < 0.5. Functional annotations and associated pathways of these DMs were determined using the KEGG compound database (http://www.kegg.jp/kegg/compound/) and KEGG pathway database (http://www.kegg.jp/kegg/pathway.html). KEGG pathways with a P-value < 0.05 were regarded as significantly enriched.

2.6. Integrated analysis of transcriptomic and metabolomic data

To identify the pathways that respond to the effects of Cd stress on the growth and development of *H. axyridis*, we conducted a comprehensive analysis integrating transcriptomic, and metabolomic data. The KEGG pathways that were enriched by DEGs and DMs in each pairwise comparison was integrated, and the shared pathways were identified. Based on these shared pathways, we established information networks and heat maps to elucidate the key pathways and biological changes that are co-regulated by genes, and metabolites.

2.7. Food-chain cadmium exposure experiment

To simulate the natural Cd exposure pathway for the *H. axyridis*, this study employed a "soil–plant–aphid" exposure system. With reference to Wang et al. [18], Cd concentrations were set at 0 (control), 3.125, 6.25, 12.5, 25, and 50 mg/kg. Cadmium chloride was used to prepare Cd^{2+} solutions at the corresponding concentrations. Broad bean seeds were soaked in the respective Cd^{2+} solutions for 24 h and then sown in a potting mixture consisting of nutrient soil, vermiculite, and perlite in a volume ratio of 12:4:2. During cultivation, each pot was irrigated every 3 days with 400 mL of the corresponding Cd^{2+} solution. After 4 weeks of growth, aphids were introduced onto the broad bean plants for feeding [19]. Subsequently, newly hatched *H. axyridis* larvae were allowed to feed on the Cd-exposed aphids. Phenotypic changes in the *H. axyridis* were monitored, and emerged adults were collected for subsequent molecular and biochemical analyses. Cadmium content in ladybugs was determined according to the method of Wan et al. [20].

2.7.1. Carbohydrate metabolism analysis

Samples were homogenized using an automated high-throughput grinder followed by ultrasonic disruption (Bioruptor UCD-200, Thermofisher Scientific). After lysis, cold PBS (4 °C) was added, and the homogenate was centrifuged at 1000 × g for 20 min to collect the supernatant. One aliquot of the supernatant was used for quantification of trehalose, glycogen, and total protein. Another aliquot was further centrifuged at 20,800 × g for 60 min at 4 °C to obtain a clarified supernatant, which was used for glucose measurement, protein assay, and soluble trehalase1 (TRE1) activity analysis. The pellet from the first centrifugation was resuspended in PBS and vortexed thoroughly to prepare a suspension for subsequent glucose, protein, and membrane-bound trehalase2 (TRE2) activity determinations. Trehalose content was measured by the anthrone method. Glycogen and glucose levels, as well as both TRE1 and TRE2 activities, were assayed using a commercial glucose assay kit (SIGMA). Total protein concentration was determined with the BCA protein assay kit (Beyotime). Quantification was based on standard curves generated for each analyte (Fig. S1). Each experiment was performed with three biological replicates.

2.7.2. qPCR analysis

Real-time polymerase chain reaction (RT-qPCR) was performed using TB Green Premix Ex Taq II (Takara Bio) on a CFX96 Touch system (Bio-Rad, Germany). Reactions contained cDNA template, gene-specific primers (Table S1 and Fig. S2), and master mix in a 20 μL volume. Cycling conditions: 95°C for 30 s; 40 cycles of 95°C for 5 s and 60°C for 20 s. Melt curve analysis confirmed amplification specificity. The *rp49* gene (GenBank: AB552923) served as the endogenous control [21]. Relative expression was calculated by the $2^{-\Delta\Delta CT}$ method.

2.8. Statistical analysis

Data are presented as mean ± SEM. One-way ANOVA with Tukey's HSD test ($P < 0.05$) or independent-sample *t*-tests (SPSS v26) were used for group comparisons. Distinct lowercase letters denote significant differences in figures (Tukey's test). Graphs were generated in GraphPad Prism 8.0 and Origin 2024 and bioinformatics (an online platform for data analysis and visualization).

3. Results

3.1. Toxicity effect of cadmium chloride on H. axyridis larvae

The dose-mortality relationship was modeled using probit regression, resulting in the equation: $y = -2.070 + 2.340x$ (where $x = \log_{10}$ [Cd concentration]) (Fig. 1A). The model showed an excellent fit to the data, as evidenced by a high coefficient of determination ($R^2 = 0.975$) and a non-significant chi-square goodness-of-fit test ($\chi^2 = 0.548$, $P = 0.969$) (Fig. 1A and Table 1). The calculated median lethal concentration (LC_{50}) was 7.667 mg/mL, the 25 % lethal concentration (LC_{25}) was 3.948 mg/mL, and the 75 % lethal concentration (LC_{75}) was 14.890 mg/mL (Table 1). Moreover, we demonstrated that cadmium accumulates in ladybugs through transfer along the soil-plant-aphid food chain (Figs. 1B and 1C), and induces significant phenotypic abnormalities, including growth retardation and morphological deformities, across all cadmium-treated groups (Fig. 1D). The results demonstrate that Cd transfer through the food web exerts a substantial toxic effect on the predator's development and morphology.

3.2. Analysis of differentially expressed genes in transcriptome

To investigate the transcriptional regulatory mechanisms of *H. axyridis* under Cd stress, we performed high-throughput RNA-Seq analysis on larvae injected with $CdCl_2$ solutions at LC_{25}, LC_{50}, and LC_{75} concentrations, alongside ddH_2O-injected controls. Compared with the control group, the number of differentially expressed genes (DEGs) was as follows: 1986 in the LC_{25} group (1264 upregulated, 722 downregulated), 1471 in the LC_{50} group (592 upregulated, 879 downregulated), and 1433 in the LC_{75} group (870 upregulated, 563 downregulated) (Fig. S3). Venn diagram analysis revealed that the LC_{25}, LC_{50}, and LC_{75} groups harbored 806, 519, and 435 unique DEGs (relative to the control), respectively, with 416 DEGs shared across all three treatment groups (Fig. 2A). Pairwise comparison between cadmium treatment groups revealed distinct patterns of differential gene expression. The number of DEGs was as follows: 1392 genes between LC_{25} and LC_{50} (519 upregulated, 873 downregulated in LC_{50}), 1392 genes between LC_{25} and LC_{75} (522 upregulated, 870 downregulated in LC_{75}), and 1174 genes between LC_{50} and LC_{75} (701 upregulated, 473 downregulated in LC_{75}) (Fig. S3). These results indicate that cadmium stress induces extensive transcriptional reprogramming in *H. axyridis* larvae.

Visualization of the top 20 significantly enriched KEGG pathways (Fig. 2B) revealed that DEGs were notably enriched in pathways including Carbohydrate Metabolism. WGCNA of all DEGs clustered them into 21 co-expression modules (Fig. 2C). Module-trait association heatmap analysis (Fig. 2D) demonstrated that transcript accumulation in the MEroyalblue module showed an opposite trend to the expression of DEGs related to several metabolic pathways in the control group such as cellular carbohydrate metabolic process, monocarboxylic acid metabolic process, including genes encoding maltase-glucoamylase, alpha,

Table 1
Toxicity test of CdCl2 on the larvae of *H. axyridis*.

Reagent	Toxicity regression equation	P(sig) value	Chi-square value	LC25 (Lethal Concentration 25)	95 % confidence interval of LC25	LC50 (Lethal Concentration 50)	95 % confidence interval of LC50	LC75 (Lethal Concentration 75)	95 % confidence interval of LC75
$CdCl_2$	y = -2.070 + 2.340x (X is the logarithm of base 10)	0.969	0.548	3.948 mg/mL	2.074–5.217	7.667 mg/mL	6.107–9.047	14.89 mg/mL	12.029–23.451

alpha-trehalase, and alpha-amylase (Fig. 2E). To validate the transcriptomic data, the expression levels of selected trehalase genes were examined by qPCR. As shown in Fig. S4, the qPCR results were consistent with the RNA-Seq trends, confirming the reliability of the sequencing data.

3.3. Differential metabolite analysis revealed an imbalance in carbohydrate metabolites in response to cadmium stress

To investigate the metabolic regulatory mechanism of *H. axyridis* under Cd stress, a widely targeted metabolomics analysis was performed using the UPLC-ESI-MS/MS system on larvae injected with $CdCl_2$ solutions at LC_{25}, LC_{50}, and LC_{75} concentrations, as well as ddH_2O. Volcano plots showed differences in primary and secondary metabolites under Cd stress. Compared with the control group, the number of differentially metabolites (DMs, VIP > 2; $P < 0.01$, n = 6) in the LC_{25}, LC_{50}, and LC_{75} treatment groups was 907 (389 upregulated, 518 downregulated), 294 (194 upregulated, 100 downregulated), and 511 (240 upregulated, 271 downregulated), respectively (Fig. 3A). Pattern analysis of DMs revealed that patterns 7, 6, 19, and 21 contained a large number of DMs; among them, 157 metabolites showed an upward trend with increasing Cd concentration, and 79 showed a downward trend (Fig. 3B). KEGG pathway enrichment analysis of DMs indicated that they were significantly enriched in pathways such as Biosynthesis of amino acids, Metabolic pathways, and Phenylalanine, tyrosine and tryptophan biosynthesis (Fig. 3C and Table S2). Among the metabolites responding to Cd stress, sucrose (Sucrose/0.663_342.1156), fucose (Fucose/0.669_164.0685), sucrose 6′-phosphate (Sucrose 6′-phosphate/0.6_422.0817), and amylose exhibited significant changes (Figs. 3D and 3E). This indicates that Cd stress also causes systemic disorders at the metabolite level, confirming the extensive nature of its toxic effects.

3.4. Multi-omics integrated analysis: Construction of a molecular regulatory model for energy metabolism disorders under cadmium stress

By integrating transcriptome and metabolome data, starch and sucrose metabolism was identified as a key pathway in response to Cd stress. Nine-quadrant plot analysis showed that for the Cd treatment groups, genes with a fold change (FC) ≥ 2 and p-value < 0.05 exhibited consistent and positively correlated change patterns with their associated metabolites, indicating that the changes in these metabolites may be positively regulated by their associated genes (Fig. 4A). Pathway enrichment analysis further revealed that cysteine and methionine metabolism, galactose metabolism, and starch and sucrose metabolism were the pathways significantly co-enriched by differentially expressed genes (DEGs) and differentially metabolites (DMs) (Fig. 4B). In the starch and sucrose metabolism pathway, 3 DEGs including alpha, alpha-trehalase, and 2 DMs including sucrose were identified (Fig. 4C, D). RT-qPCR was used to verify the expression levels of trehalase genes in *H. axyridis* from the transcriptome data, and the expression patterns of 7 genes were basically consistent between the two detection methods (Fig. S4), confirming the reliability of the transcriptome sequencing results. To further dissect the regulatory associations between key DEGs and DMs in the starch and sucrose metabolism pathway, a gene-metabolite correlation network analysis was performed based on Spearman's correlation coefficients (Fig. 4E). The results demonstrated that *TRE1–2* was significantly positively correlated with multiple metabolites including Histamine, Galactose-1-phosphate and Phosphoric acid, indicating that the expression dynamics of *TRE1–2* were highly consistent with the accumulation trends of these metabolites. In contrast, *TRE2–1* and trehalose-6-phosphate synthase (*TPS*) both showed a significant negative correlation with histamine, suggesting that the trehalose catabolic and anabolic pathways may exhibit opposite regulatory trends under Cd stress. Notably, a negative correlation was also observed between *TRE1–2* and *TPS*, which implies an antagonistic regulatory relationship between trehalose synthesis (mediated by *TPS*) and decomposition (mediated by *TRE1–2*) during Cd-induced metabolic reprogramming. Considering that trehalase is an enzyme that decomposes trehalose in insects, and trehalose metabolism plays a key role in insect growth and development, subsequent experiments were designed to explore the effect of Cd exposure on trehalose metabolism in *H. axyridis*.

3.5. Effects of cadmium stress on gene expression, enzyme activity, and sugar content in the trehalose metabolic pathway

To further explore the impact of Cd stress on trehalose metabolism, indicators related to sugar content in *H. axyridis* feeding on Cd-contaminated aphids were determined. Compared with the control group, the trehalose content in all five Cd treatment groups (3.125, 6.25, 12.5, 25, 50 mg/kg) decreased, with significant reductions observed in the 3.125, 6.25, and 12.5 mg/kg groups. Glycogen and glucose contents in Cd treatment groups were generally lower than those in the control group, with significant differences in all groups except the 50 mg/kg group (Fig. 5A-C). After Cd treatment, the activity of soluble trehalase was significantly lower than that in the control group (Fig. 5D). The activity of membrane-bound trehalase was also significantly reduced in the 12.5 and 25 mg/kg treatment groups (Fig. 5E). Gene expression analysis revealed that *TRE1–1* was significantly downregulated in the 3.125, 6.25, and 25 mg/kg groups but upregulated in the 12.5 mg/kg group. *TRE1–3* expression was significantly increased in the 12.5 mg/kg group but decreased in the 25 mg/kg group (Fig. 5F). *TRE2* was downregulated across all treatment groups, while *TRE2-like* was significantly downregulated specifically in the 12.5 mg/kg group. *TPS* expression was significantly upregulated in the 3.125 and 50 mg/kg groups but downregulated in the 6.25 and 25 mg/kg groups (Fig. 5G).

4. Discussion

Heavy metal Cd (Cd) pollution poses a severe threat to the stability of agricultural ecosystems, particularly by impairing the population health of natural enemies like *Harmonia axyridis* a key biological control agent for pests [22,23]. To clarify the toxic effects of Cd on *H. axyridis* and its intrinsic mechanisms, this study systematically integrated toxicological testing, transcriptomics, metabolomics, and molecular validation. The findings, closely aligned with the results of each analytical phase, confirm that 3rd instar *H. axyridis* larvae are highly sensitive to Cd (LC_{50} = 7.667 mg/mL for $CdCl_2$); Cd stress primarily disrupts carbohydrate

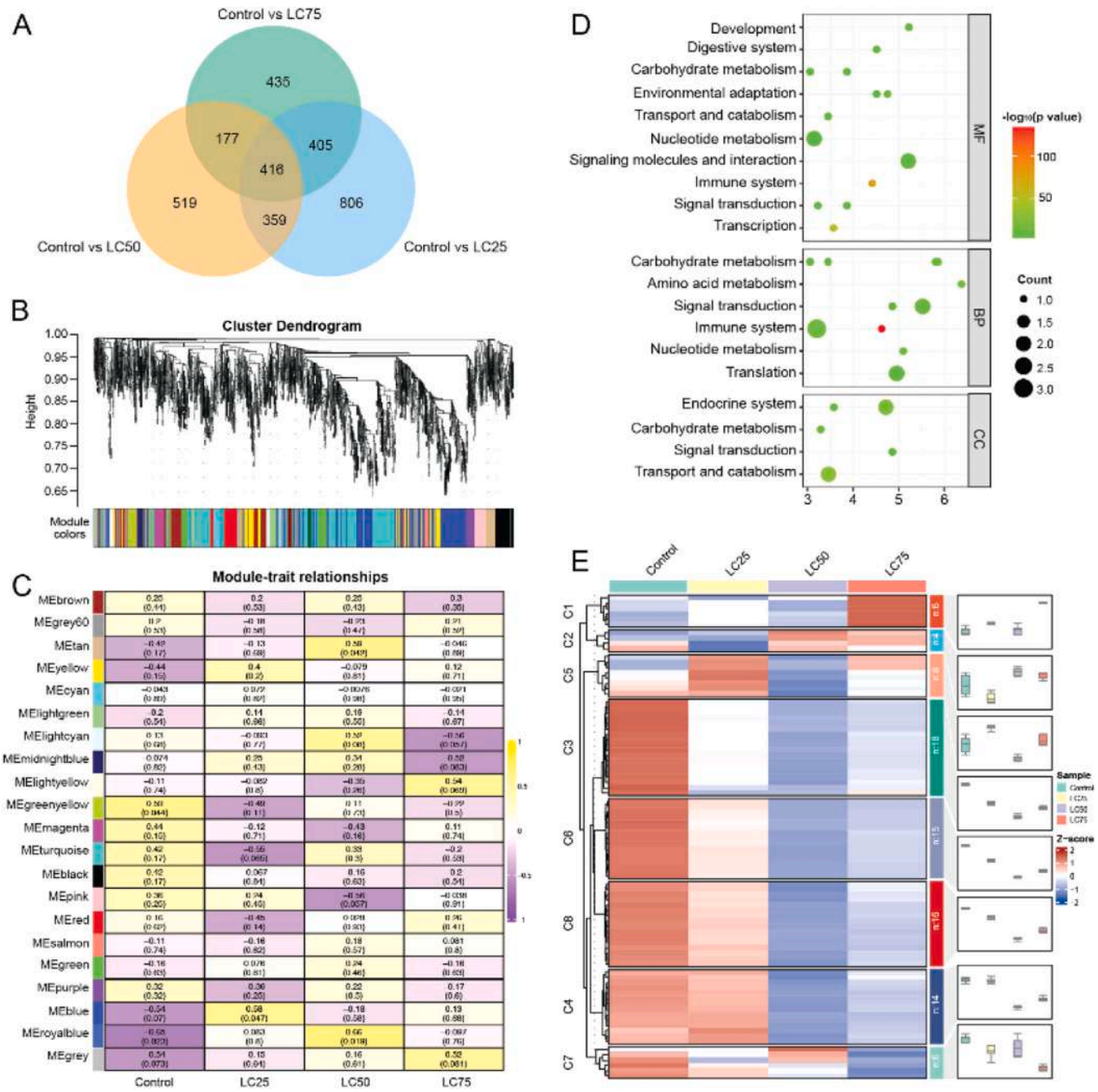

Fig. 2. Results of transcriptome sequencing analysis. (A) Venn diagram of differentially expressed genes (DEGs) in different cadmium treatment concentration groups. (B) Bubble plot of the top 20 KEGG pathways significantly enriched with DEGs. (C) Dendrogram of gene co-expression modules obtained from WGCNA analysis (each color represents a module). (D) Module-trait association heatmap. The color of the heatmap represents the correlation coefficient (yellow: positive correlation; purple: negative correlation), and the closer the value is to |1|, the stronger the correlation. The numbers in parentheses are the corresponding p-values. (E) Heatmap of expression trends of DEGs related to key metabolic pathways in the MEroyalblue module under different cadmium treatment concentrations (showing expression patterns compared with the control group).

metabolism especially starch-sucrose and trehalose metabolism and amino acid biosynthesis; and the core toxic mechanism relies on a "gene-metabolite" regulatory network centered on trehalase down-regulation and trehalose decomposition blockage.

Consistent with the toxicological results (Fig. 1A), the LC_{50} of Cd 3rd instar larvae of *H. axyridis* larvae (7.667 mg/mL) is lower than that of *Coccinella septempunctata* [24], a congeneric *H. axyridis* widely used in biological control, indicating higher Cd sensitivity in *H. axyridis*. This sensitivity is not only prominent among ladybug species but also in comparison with other predatory natural enemies. Such high sensitivity implies that *H. axyridis* populations face greater survival pressure in Cd-contaminated farmlands. As shown in the phenotypic observation results (Fig. 1B), Cd exposure induces dose-dependent abnormalities such as developmental arrest and body teratogeny, with the LC_{75} group showing 42 % higher mortality and 37 % more teratogenic individuals than the LC_{25} group.

These phenotypic damages are not random but stem from physiological dysfunction: the developmental arrest directly correlates with the blocked carbohydrate catabolism observed in metabolic results, which leads to insufficient energy supply; while body teratogeny is

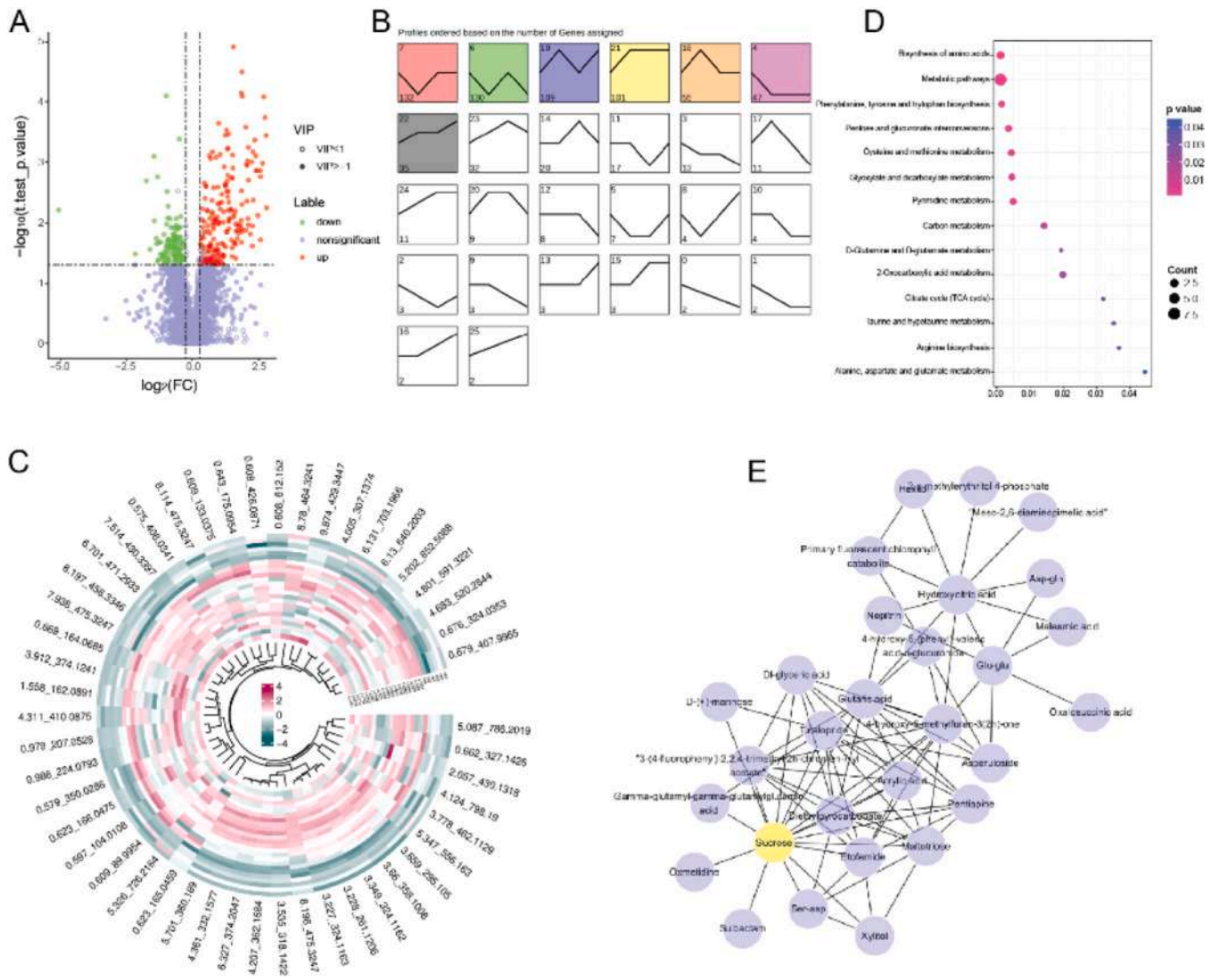

Fig. 3. Results of metabolomics analysis. (A) Volcano plots of differentially metabolites (DMs) under different cadmium treatment concentrations (green: down-regulated; red: upregulated; purple-gray: no difference). Criteria for DM screening: 1) VIP $\geq$ 1 in the PLS-DA model; 2) fold change $\geq$ 2 or $\leq$ 0.5) p-value $<$ 0.05. (B) Clustering of expression patterns and quantity statistics (upward/downward trends) of DMs under different cadmium concentrations. (C) Bubble plot of KEGG pathways significantly enriched with DMs. (D) Expression heatmap of key differential metabolites under different cadmium treatment concentrations. (E) Protein-protein interaction (PPI) network diagram of key differential metabolites.

linked to disrupted amino acid biosynthesis (Fig. 3C) which impairs protein synthesis. This observation aligns with studies on herbivorous and aquatic insects such as *Tramea cophysa*, *Spodoptera litura*, and species of *Trichogramma*, which confirm that heavy metals induce insect growth retardation by impairing core physiological processes [25,10, 26]. However, our study extends this conclusion to predatory natural enemies and highlights a trophic level-specific difference. Compared with herbivorous insects that often show generalized metabolic disorders under Cd stress [27], *H. axyridis* exhibits a more focused disruption on energy metabolism pathways, reflecting the unique physiological adaptation characteristics of predatory insects with high energy demand for predation and movement.

The transcriptomic enrichment results (Fig. 2B) clearly show that carbohydrate metabolism is the most significantly disrupted pathway, confirming Cd's targeted interference with *H. axyridis*' energy supply system, consistent with previous findings that heavy metals disrupt insect glycolysis, TCA cycle, and sugar metabolism [5,27]. However, our study reveals a more specific mechanism than prior research on herbivorous insects. For instance, Jiang et al [5]. reported that Cd down-regulates *GAPC* and *Idh1* (key glycolysis genes) in *Lymantria dispar*, a herbivore, focusing on general glycolytic flux inhibition. In contrast, our WGCNA results (Fig. 2D) identifies the MEroyalblue module as the core regulatory module for Cd-induced energy disorders, and the module's key genes including maltase-glucoamylase and α, α-trehalase (Fig. 2E) specifically target starch-sucrose and trehalose metabolism. This targeted disruption of trehalose metabolism, an insect-specific core energy pathway, is a novel insight into heavy metal toxicity in predatory insects, which differs from the reported Cd-induced disruption of fatty acid metabolism in *Apis mellifera*, a pollinator [28] .Notably, the down-regulation of these catabolic genes shows a distinct dose-dependent trend consistent with the transcriptomic data (Fig. 2E): α,α-trehalase expression in the LC_{75} group is only 35 % of the control, while the LC_{25} group retains 62 % of the control level. This dose dependence directly explains the concentration-dependent severity of phenotypic damage, as higher Cd concentrations further suppress gene expression, exacerbating energy shortage.

The metabolomic results (Figs. 3D, 3E) provide direct evidence for this metabolic blockage: 157 differentially metabolites (DMs) are upregulated, including sucrose and sucrose 6'-phosphate which are upstream substrates of carbohydrate catabolism, while 79 DMs are

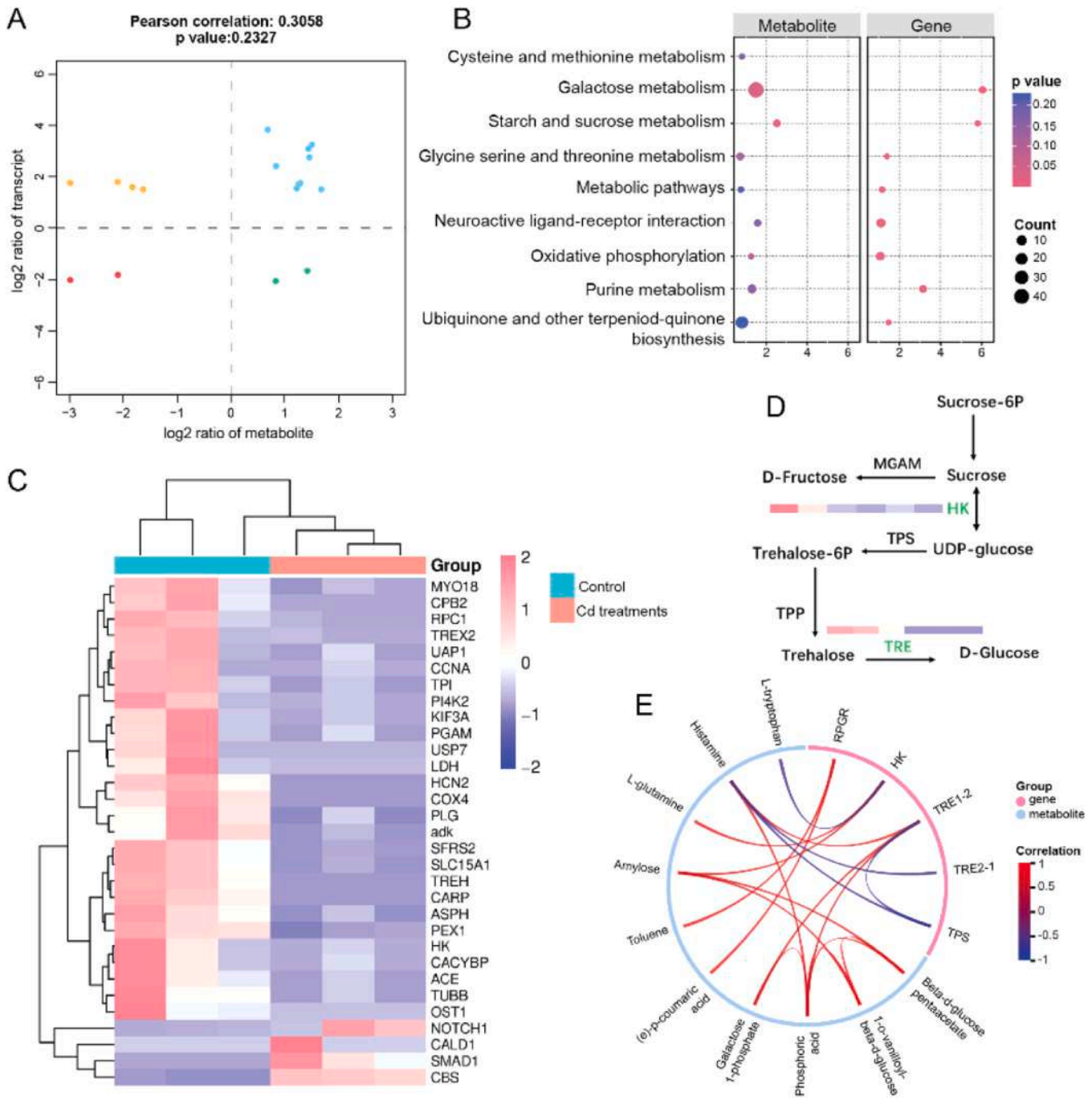

Fig. 4. Results of integrated transcriptome and metabolome analysis. (A) Nine-quadrant plot of gene-metabolite associations (showing the expression change patterns and correlations of associated pairs in the control and cadmium treatment groups). (B) Bubble plot of KEGG pathways significantly co-enriched by DEGs and DMs. (C) Starch and sucrose metabolism pathway map, with key DEGs and DMs labeled. (D) Expression heatmap of key DEGs and DMs in the starch and sucrose metabolism pathway under different cadmium treatment concentrations. (E) Gene-metabolite correlation network diagram (chord diagram). This chord diagram displays the Spearman correlations between DEGs and DMs screened from the starch and sucrose metabolism pathway. Key metabolites and metabolism-related genes are labeled in pink on the outer ring of the diagram. The chord lines connecting metabolite-gene pairs indicate significant correlations, where blue represents negative correlation and red represents positive correlation, with correlation coefficient values ranging from –1 to + 1.

downregulated, such as amylose which is an energy storage compound. Functional clustering of these DMs based on KEGG enrichment shows that upregulated metabolites are mainly enriched in starch-sucrose metabolism, amino acid biosynthesis, and stress response pathways: sucrose accumulation (2.8-fold higher in LC_{75} vs. control) directly reflects blocked trehalose decomposition; the upregulation of amino acid biosynthesis metabolites may be a compensatory response to Cd-induced protein damage; and stress response metabolites such as proline accumulate to mitigate osmotic stress. In contrast, the downregulation of amylose and glycogen which are energy storage compounds is a direct result of insects decomposing stored energy to compensate for glucose shortage, forming a "substrate accumulation-storage depletion" metabolic signature that confirms carbohydrate catabolism blockage.

Following Cd exposure, the DMs in *H. axyridis* were mainly enriched in amino acid biosynthesis and carbohydrate metabolism pathways

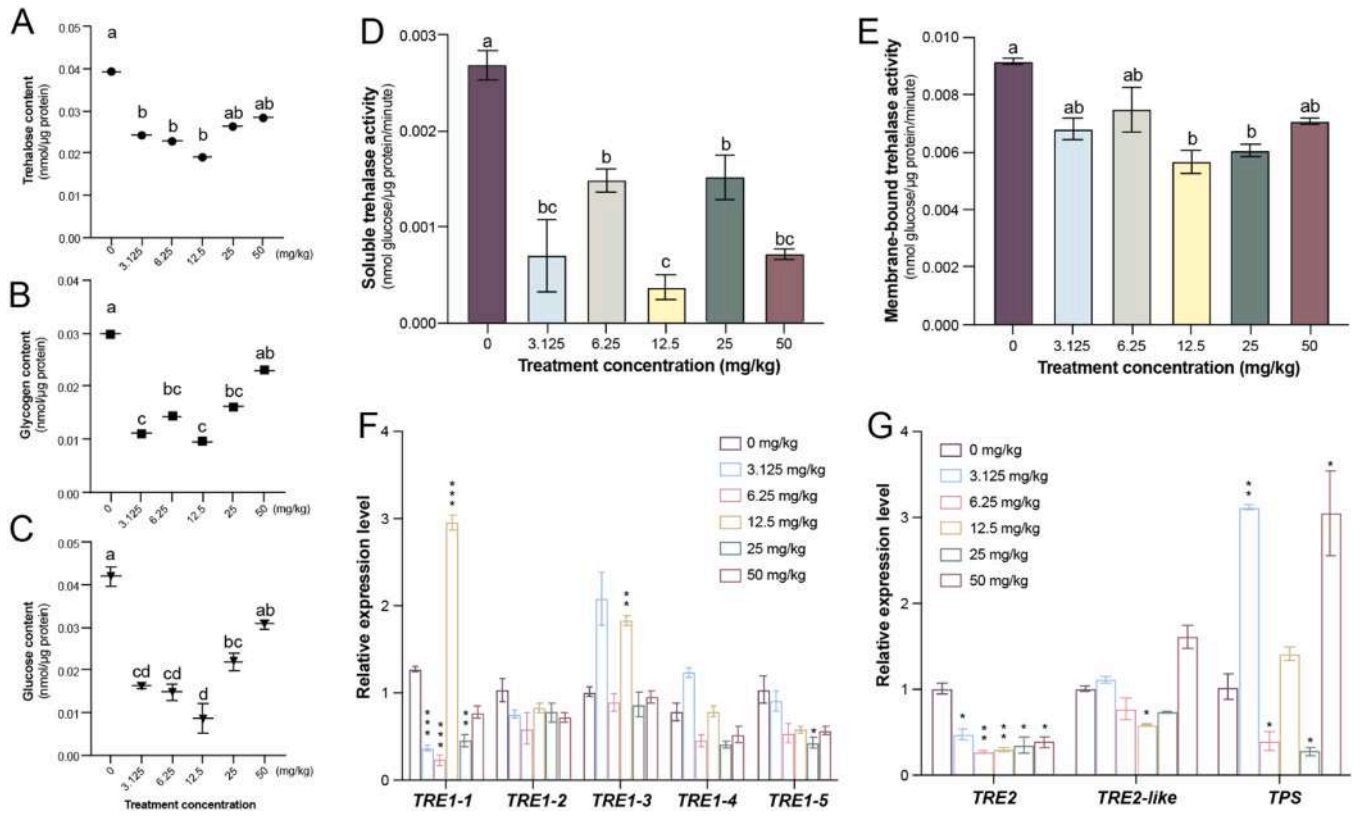

Fig. 5. Effects of cadmium stress on related indicators of the trehalose metabolic pathway in *H. axyridis*. (A-C) Trehalose, glycogen, and glucose contents in the cadmium treatment groups. (D-E) Activities of soluble trehalase and membrane-bound trehalase. (F-G) Expression levels of trehalase (T RE) and trehalose-6-phosphate synthase (*TPS*) genes. Values with different letters are significantly different at $P < 0.05$. Data are presented as mean ± SEM, (n = 3). "**", $P < 0.01$; "*", $P < 0.05$; "ns", $P > 0.05$.

(Fig. 3E). Insect energy metabolism relies on pathways including glycolysis, the tricarboxylic acid (TCA) cycle, and amino acid metabolism [11], and heavy metal stress has been confirmed to disrupt these pathways [6,27]. The results of this study further support the hypothesis that Cd may impair the physiological functions of *H. axyridis* by interfering with the core pathways of energy metabolism.

The 90 % consistency between DEGs and DMs (Fig. 4A) further strengthens the causal link between gene downregulation and metabolic disorders: the transcriptomic downregulation of trehalose metabolism genes directly drives the accumulation of sucrose and other metabolites observed in metabolomics (Fig. 4D). The starch-sucrose metabolism pathway (Fig. 4B) is identified as the core response pathway, with α,α-trehalase downregulation (Fig. 4C) being the key trigger for trehalose decomposition blockage. Trehalose is the main energy source in insect hemolymph [29], the abnormal expression of *TRE1–3*, upregulated in the LC_{25} group but downregulated in LC_{50} and LC_{75} groups, can be explained by a stress compensation mechanism: under low Cd concentrations, *H. axyridis* transiently upregulates *TRE1–3* to compensate for reduced activity of other trehalase isoforms such as *TRE1–2* and *TRE2–1*, attempting to maintain trehalose decomposition; however, high Cd concentrations exceed the compensation capacity, leading to universal downregulation.

The enzyme activity results (Figs. 5D, 5G) further validate the disruption of the trehalose pathway. Cd exposure significantly reduced TRE1 activity, and membrane-bound TRE2 activity was also notably suppressed in several treatment groups. For instance, soluble TRE activity decreased progressively relative to the control across increasing exposure levels. Building upon evidence from toxicological, transcriptomic, metabolomic, and enzymatic assays, we propose that Cd impairs *H. axyridis* primarily by disrupting trehalose-mediated energy homeostasis. Specifically, Cd downregulates key *TRE2* and inhibits TRE2 activity, which blocks trehalose decomposition, limits glucose availability, and ultimately leads to energy deficiency, growth arrest, and phenotypic abnormalities. The upregulation of *TRE1–3* observed at 12.5 mg/kg may represent a compensatory response under moderate stress. This mechanism is consistent with Wu et al [30]. 's observation that heavy metals act by disrupting core metabolic pathways in insects, but specifies trehalose metabolism as the key target in predatory insects, which complements the existing understanding of heavy metal toxicity mechanisms across different insect trophic levels. The practical value of these findings is closely tied to agricultural ecosystem protection and can be benchmarked against existing studies on natural enemy protection in polluted areas. The LC_{50} (7.667 mg/mL) and LC_{25} (3.948 mg/mL, corrected to match results section) values from toxicological results can serve as more sensitive biological indicators for Cd pollution risk assessment compared with traditional indicators such as earthworms (LC_{50} = 20.5 mg/mL [21]). When environmental Cd exceeds LC_{25}, *H. axyridis* population stability and biological control capacity are significantly impaired, which provides a more precise threshold for ecological risk early warning in farmlands.

Despite these insights, this study has limitations linked to its experimental design, which are also common in related insect heavy metal studies but require attention. The research focused solely on 3rd instar larvae, and results may not apply to other developmental stages including eggs, pupae and adults. As shown in preliminary observations, adult *H. axyridis* show lower mortality than larvae, a stage-specific sensitivity that has also been reported in *C. septempunctata* [26]. The toxicity mechanism is inferred from multi-omics correlations, and direct evidence such as RNAi-mediated trehalase knockout is needed to verify the causal link between trehalase downregulation and energy shortage. Future studies should address these limitations by expanding to multiple developmental stages and long-term exposure scenarios, and using

molecular tools such as RNAi to validate trehalase's regulatory role.

In conclusion, this study systematically reveals the Cd toxicity mechanism of *H. axyridis* centered on trehalose metabolism disruption, which not only complements the knowledge gap of heavy metal toxicity on predatory natural enemies but also provides a theoretical basis for the protection of natural enemy resources in Cd-polluted agricultural ecosystems. The comparative analysis with other insect species highlights the trophic level-specific response characteristics of *H. axyridis*, which is of great significance for improving the accuracy of ecological risk assessment and the effectiveness of biological control in heavy metal-polluted areas.

5. Conclusion

This research provides mechanistic insights into Cd toxicity in *H. axyridis*. The key finding is that Cd stress specifically perturbs core carbohydrate metabolic pathways, as evidenced by the co-enrichment of differential genes and metabolites in starch/sucrose and galactose metabolism. This work not only advances our understanding of heavy metal toxicity in beneficial arthropods but also identifies potential molecular targets for assessing ecological risks in agricultural systems.

Environmental implication

Cadmium (Cd), as a ubiquitous heavy metal pollutant, poses a potential threat to the ecological functions of the natural enemy insect *Harmonia axyridis*, but the molecular mechanism underlying its toxic effects remains unclear. In this study, a multi-omics approach combining transcriptomics and metabolomics was employed to systematically analyze the molecular responses of *H. axyridis* under cadmium stress. The results showed that differentially expressed genes (DEGs) and differential metabolites (DEMs) were co-enriched in the starch and sucrose metabolism pathway when comparing Cd-treated groups with controls. And cadmium stress significantly inhibited the expression of key genes in the starch and sucrose metabolism pathway. In conclusion, the downregulation of gene expression led to the accumulation of key carbohydrates such as trehalose, causing energy supply disorders, which may be the key mechanism mediating the toxic effects of cadmium on *H. axyridis*. The findings of this study reveal a new mechanism by which heavy metal pollution affects natural enemy insects.

CRediT authorship contribution statement

Min Zhou: Investigation, Data curation. **Jie Wang:** Validation, Investigation, Data curation. **Bin Tang:** Writing – review & editing, Supervision, Funding acquisition. **Li yan:** Writing – review & editing, Supervision, Conceptualization. **Shasha Wang:** Writing – review & editing, Writing – original draft. **Sijing Wan:** Writing – review & editing, Software, Data curation. **Lei Yue:** Validation, Supervision, Methodology. **Qintian Shen:** Methodology, Investigation, Formal analysis.

Declaration of Competing Interest

The authors declare that they have no known competing financial interests or personal relationships that could have appeared to influence the work reported in this paper.

Acknowledgements

This work was supported by National Natural Science Foundation of China (3250170142) and the China Postdoctoral Science Foundation (2025M772658).

Appendix A. Supporting information

Supplementary data associated with this article can be found in the online version at doi:10.1016/j.jhazmat.2026.141412.

Data availability

Data will be made available on request.

References

[1] Alengebawy, A., Abdelkhalek, S.T., Qureshi, S.R., et al., 2021. Heavy metals and pesticides toxicity in agricultural soil and plants: ecological risks and human health implications. Toxics 9 (3), 42. https://doi.org/10.3390/toxics9030042.
[2] Gao, S., Zheng, F., Yue, L., et al., 2024. Chronic cadmium exposure impairs flight behavior by dampening flight muscle carbon metabolism in bumblebees. J Hazard Mater 466, 133628. https://doi.org/10.1016/j.jhazmat.2024.133628.
[3] El Rasafi, T., Oukarroum, A., Haddioui, A., et al., 2022. Cadmium stress in plants: A critical review of the effects, mechanisms, and tolerance strategies. Crit Rev Environ Sci Tec 52 (5), 675–726. https://doi.org/10.1080/10643389.2020.1835435.
[4] Genchi, G., Sinicropi, M.S., Lauria, G., et al., 2020. The effects of Cadmium toxicity. Int J Environ Res Public Health 17 (11), 3782. https://doi.org/10.3390/ijerph17113782.
[5] Jiang, D., Zhou, Y., Tan, M., et al., 2020. Cd exposure-induced growth retardation involves in energy metabolism disorder of midgut tissues in the gypsy moth larvae. Environ Pollut 266 (3), 115173. https://doi.org/10.1016/j.envpol.2020.115173.
[6] Zheng, L., Tan, M., Yan, S., et al., 2023. Cadmium exposure-triggered growth retardation in *Hyphantria cunea* larvae involves disturbances in food utilization and energy metabolism. Ecotoxicol Environ Saf 256, 114886. https://doi.org/10.1016/j.ecoenv.2023.114886.
[7] Płachetka-Bożek, A., Kafel, A., Augustyniak, M., 2018. Reproduction and development of *Spodoptera exigua* from cadmium and control strains under differentiated cadmium stress. Ecotoxicol Environ Saf 166, 138–145. https://doi.org/10.1016/j.ecoenv.2018.09.016.
[8] Shen, Q., Wang, S., Wan, S., Guan, M., et al., 2025. Effects of Cadmium Accumulation Along the Food Chain on the Fitness of *Harmonia axyridis*. Agronomy 15 (5), 1261. https://doi.org/10.3390/agronomy15051261.
[9] Hu, X., Fu, W., Yang, X., et al., 2019. Effects of cadmium on fecundity and defence ability of *Drosophila melanogaster*. Ecotoxicol Environ Saf 171, 871–877. https://doi.org/10.1016/j.ecoenv.2019.01.029.
[10] Wang, J., Di, N., Wang, C.X., Zhu, Z.Y., Prager, S.M., Huang, H.X., Trumble, J.T., Desneux, N., Li, Y.X., Wang, S., et al., 2025. Transgenerational effects of heavy metal contamination on two *Trichogramma* egg parasitoids and potential impacts on biological control. Insect Sci 7. https://doi.org/10.1111/1744-7917.70125.
[11] Wang, J., Hussain, T., Duan, Y., et al., 2022. Editorial: Nutritional management for the energy metabolism in animals. Front Vet Sci 9, 900736. https://doi.org/10.3389/fvets.2022.900736.
[12] Saska, P., Özgökçe, M.S., Skuhrovec, J., et al., 2021. Bias introduced by the simplified method for the estimation of the intrinsic rate of increase of aphid populations: A meta-analysis. Entomol Gen 41, 305–316. https://doi.org/10.1127/entomologia/2021/1190.
[13] Jing, X.H., Ali, J., Jianye, Z., et al., 2025. Prior Brassica rapa infestation by the cabbage bug, *Eurydema ornata* alters the performance and behavior of the peach-potato aphid, *Myzus persicae* and its natural enemies. Pest Manag Sci 28. https://doi.org/10.1002/ps.8921.
[14] Naikoo, M.I., Raghib, F., Dar, M.I., et al., 2021. Uptake, accumulation and elimination of cadmium in a soil - Faba bean (*Vicia faba*) - Aphid (*Aphis fabae*) - Ladybird (*Coccinella transversalis*) food chain. Chemosphere 279, 130522. https://doi.org/10.1016/j.chemosphere.2021.130522.
[15] Shi, Z., Wang, S., Pan, B., et al., 2022. Effects of zinc acquired through the plant-aphid-ladybug food chain on the growth, development and fertility of *Harmonia axyridis*. Chemosphere 259, 127497. https://doi.org/10.1016/j.chemosphere.2020.127497.
[16] Luo, Y.J., Chen, Y., Wang, X.J., et al., 2022. Validamycin affects the development and chitin metabolism in *Spodoptera frugiperda* by inhibiting trehalase activity. Entomol Gen 42, 931–939. https://doi.org/10.1127/entomologia/2022/1608.
[17] Malematja, E., Manyelo, T.G., Sebola, N.A., et al., 2023. The accumulation of heavy metals in feeder insects and their impact on animal production. Sci Total Environ 885, 163716. https://doi.org/10.1016/j.scitotenv.2023.163716.
[18] Wang, X., Zhang, C., Qiu, B., et al., 2017. Biotransfer of Cd along a soil-plant-mealybug-ladybird food chain: A comparison with host plants. Chemosphere 168, 699–706. https://doi.org/10.1016/j.chemosphere.2016.11.005.
[19] Xie, Y., Wang, S., Wan, S., et al., 2024. The stress response of aphids to the accumulation of heavy metals along *Vicia faba* L. under cadmium treatment. Insects 15 (12), 999. https://doi.org/10.3390/insects15120999.
[20] Wan, S., Wang, S., Li, Y., et al., 2025. *Megoura crassicauda* promote the ability of *Vicia faba* L. to remediate cadmium pollution of water and soil. Ecotoxicol Environ Saf Ecotoxicol Environ Saf 290, 117777. https://doi.org/10.1016/j.ecoenv.2025.117777.
[21] Yang, X., Pan, H., Yuan, L., et al., 2018. Reference gene selection for RT-qPCR analysis in *Harmonia axyridis*, a global invasive lady beetle. Sci Rep 8 (1), 2689. https://doi.org/10.1038/s41598-018-20612-w.
[22] Li, C., Yu, J., Mao, R., et al., 2024. Functional and numerical responses of *Harmonia axyridis* (Coleoptera: Coccinellidae) to *Rhopalosiphum nymphaeae* (Hemiptera: Aphididae) and their potential for biological control. Insects 15 (9), 633. https://doi.org/10.3390/insects15090633.

[23] Wang, S., Li, Q., Li, Y., et al., 2024. Stress response of aphid population under combined stress of cadmium and lead and its effects on development of *Harmonia axyridis*. Int J Mol Sci 25 (20), 11145. https://doi.org/10.3390/ijms252011145.
[24] Green, I.D., Diaz, A., Tibbett, M., 2010. Factors affecting the concentration in seven-spotted ladybirds (*Coccinella septempunctata* L.) of Cd and Zn transferred through the food chain. Environ Pollut 158 (1), 135–141. https://doi.org/10.1016/j.envpol.2009.07.032.
[25] Akhtar, Z.R., Tariq, K., Mavian, C., et al., 2021. Trophic transfer and toxicity of heavy metals from dengue mosquito *Aedes aegypti* to predator dragonfly *Tramea cophysa*. Ecotoxicology 30 (6), 1108–1115. https://doi.org/10.1007/s10646-021-02448-9.
[26] Zhou, J., Chen, J., Shu, Y., et al., 2021. Lead stress affects the reproduction of *Spodoptera litura* but not by regulating the vitellogenin gene promoter. Ecotox Environ Safe 208, 111581. https://doi.org/10.1016/j.ecoenv.2020.111581.
[27] Chen, J., Guo, Y., Huang, S., et al., 2021. Integration of transcriptome and proteome reveals molecular mechanisms underlying stress responses of the cutworm, *Spodoptera litura*, exposed to different levels of lead (Pb). Chemosphere 283, 131205. https://doi.org/10.1016/j.chemosphere.2021.131205.
[28] Burden, C.M., Morgan, M.O., Hladun, K.R., et al., 2019. Acute sublethal exposure to toxic heavy metals alters honey bee (*Apis mellifera*) feeding behavior, 12 Sci Rep 9 (1), 4253. https://doi.org/10.1038/s41598-019-40396-x.
[29] Lu, W., Liu, Y., Guan, R., et al., 2025. Effects of copper-based fungicides on the growth and tolerance of *Helicoverpa armigera*: implications for pest management. Pest Biochem Physiol 208, 106297. https://doi.org/10.1016/j.pestbp.2025.106297.
[30] Wu, Z., Yan, C., Xing, K., et al., 2024. Membrane-bound trehalase enhances cadmium tolerance by regulating cell apoptosis in *Neocaridina denticulata* sinensis. Sci Total Environ 944, 173798. https://doi.org/10.1016/j.scitotenv.2024.173798.